INFLUENCE OF VARIABLE THERMAL CONDUCTIVITY AND THERMAL RADIATION ON SLIP FLOW AND HEAT TRANSFER OF MHD POWER-LAW FLUID OVER A POROUS SHEET

SABA JAVAID[a,], ASIM AZIZ[b,1]

[a]School Natural Sciences, National University of Sciences and Technology, Islamabad, H-12, 45000, Pakistan

[b]College of Electrical and Mechanical Engineering, National University of Sciences and Technology, Rawalpindi, 46070, Pakistan

In this paper, the problem of boundary layer flow and heat transfer of MHD power-law fluid over a porous sheet in the presence of partial slip is investigated numerically. We assume a temperature dependent thermal conductivity and slip conditions are employed in terms of shear stress. The suitable similarity transformations are used, to transform the governing partial differential equations (PDEs) into a system of nonlinear ordinary differential equations (ODEs). The resulting system of ODEs is solved numerically using Matlab bvp4c solver. The numerical values obtained for the velocity and temperature depend on power-law index, slip parameters, permeability, suction/injection parameter, Prandlt number and Nusselt number. The effects of various parameters on the flow and heat transfer characteristics are presented through graphs and tables and discussed from physical point of view.

Keywords: Power-law fluid; Porous medium; Porous plate; Heat transfer; Partial slip; Thermal radiation; Variable thermal conductivity

1 Introduction

The layer of fluid that flows adjacent to its bounding surface is called the boundary layer. The boundary layer flow play vital role in many aspects of fluid mechanics and has been studied extensively. The applications of boundary layer theory include, the calculation of friction drag of a flat plate, a ship, an airfoil, the body of an airplane or a turbine blade, cooling devices etc. Prandtl [1] first introduced the concept of boundary layer to understand the flow behavior of fluid near a solid boundary. Blasius [2] solved the famous boundary layer equation for a flat moving plate problem and found a power series solution of the model. In the theory of non-Newtonian fluid this concept was introduced by [3]. A comprehensive literature survey on boundary layer theory and related topics can be found in the studies of [4–6].

In recent years, boundary layer models include the analysis of heat transfer because these type of processes exist in nature and have industrial applications like heat exchanger, recovery of petroleum resources, fault zones, catalytic reactors, cooling devices, chemical reactions in a reactor chamber, deposition of chemical vapor on surfaces etc. A detailed literature on forced/natural convection of viscous fluids past their bounding surface can be found in the books of [7, 8]. Kumari *at el.* in [9] first investigated the non-Darcian effects on forced convection heat transfer over a flat plate in a highly porous medium. A computational analysis of heat transfer in case of forced convection fluid flow on a heated flat plate embedded in a porous medium is performed by Luna and Mndez [10]. Khaled and Vafai [11] discussed various flow models in porous medium with applications in biological areas such as diffusion in brain tissues, tissue generation process, blood flow in tumors, bio-heat transfer in tissues and bio-convection. The interaction of free convection with thermal radiation of a fluid along with moving plate was studied by Makinde [12]. Ibrahim *et al.* in [13] examined the influence of viscous dissipation and radiation on unsteady, MHD and mixed convection flow of micropolar fluids. The effect of variable thermal conductivity on a flow of power-law fluids over stretching sheet with heat transfer was studied by Datti and N.Mahesha [14].

It is revealed from the available literature, researchers extensively studied flow models including heat transfer analysis for different geometries influenced by a number of factors including

[1]Corresponding Author Email: aaziz@ceme.nust.edu.pk

fluid viscosity, bounding surface characteristics and external forces to name a few. Limited attention was given to the slip boundary condition. Wall slip has far-reaching implications on many branches of science, engineering and industry. These include rheometric measurements, material processing, and fluid transportation [15, 16]. These studies provide a reasonable justification to apply the partial slip boundary condition relating to the shear rate at the boundary. Beavers and Joseph [17] first proposed a slip flow condition at the boundary. Since then, there has been a revival of interest in flow problems with slip conditions. In [18–21] authors employed slip boundary conditions on a forced convective boundary layer flow with heat and mass transfer of an incompressible fluid past a porous plate embedded in a porous medium.

There are fluids those exhibit complex structures which cannot be studied from the theory of Newtonian fluids. The efforts have been directed towards understanding the flow and heat transfer characteristics of non-Newtonian fluids. It is beyond the scope of this work to revisit the vast amount of literature on the boundary layer flow of different non-Newtonian fluid models. Limited work on the topic can be referred as examples in [22–24]. The power-law viscosity model of non Newtonian fluid is one in which the shear stress varies according to a power function of the strain rate. The power-law model is found to be good in representing pseudo-plastic behavior of fluids. Acrivos *et al.* [25] studied the boundary layer flow of power-law fluid past a horizontal flat plate including heat transfer. Schowalter [26] formulated the two and three dimensional boundary layer equations and found some new solutions for the equations. Andersson *et al.* [27] examined the boundary layer flow of electrically conducting power-law fluid in the presence of transverse magnetic field. Recent additions considering flow of non-Newtonian power-law fluid with heat and mass transfer under different physical situations are given by [28–31].

In aforementioned investigations, the thermophysical properties of the ambient fluid were assumed to be constant with constant thermal conductivity. However many processes in engineering occur at high temperature and it is well known that these properties may change with temperature. Moreover, knowledge on radiation heat transfer becomes very important for design of reliable equipment, nuclear plants, gas turbines and various propulsion devices or aircraft, missiles, satellites and space vehicles. On the basis of these applications, radiation effect on flow and heat transfer problems with variable thermophysical properties has become important industrially. Several publications are available on effect of radiation on flow and heat transfer (see for example [32–35])

In this publication, we show that the key parameters like, power-law index, velocity/thermal slip, thermal conductivity and thermal radiation greatly affect the thickness of momentum and thermal boundary layer. The governing partial differential equations are transformed into a system of non-linear ordinary differential equations by applying a suitable similarity transformations. These equations are then solved numerically using Matlab bvp4c solver. The numerical results are discussed for various physical parameters effecting the flow and heat transfer.

2 Problem statement and mathematical formulation

Consider the steady two-dimensional laminar flow with heat transfer of an incompressible power-law fluid under the influence of magnetic field and thermal radiation, over a semi-infinite porous plate in a porous medium. The applied magnetic field B is acting normal to the plate and induced magnetic field is considered negligible as compared to applied magnetic field because the Reynolds number for the flow is taken to be small. The surface of the plate is insulated and admits partial slip condition. The leading edge of the plate is at $x = 0$ and coincide with the plane $y = 0$. The temperature of the plate is T_w and the flow far away from the plate is uniform and in the direction parallel to the plate. The velocity and temperature far away from the plate are U_∞ and T_∞ respectively. The geometry of the flow model is given in figure (1). The governing equations under boundary layer approximation for the problem along with the

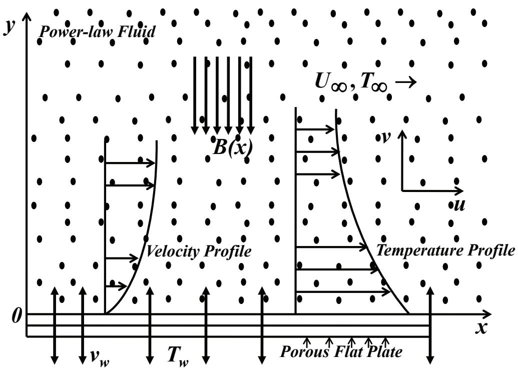

Figure 1: Geometry of the problem

slip boundary conditions can be written as

$$\frac{\partial u}{\partial x}+\frac{\partial v}{\partial y}=0, \tag{1}$$

$$u\frac{\partial u}{\partial x}+v\frac{\partial u}{\partial y}=\frac{1}{\rho}\frac{\partial \tau_{xy}}{\partial y}-\frac{1}{\rho A}(u-U_\infty)-\frac{\sigma B^2}{\rho}(u-U_\infty), \tag{2}$$

$$u\frac{\partial T}{\partial x}+v\frac{\partial T}{\partial y}=\frac{1}{\rho C_p}\left(\frac{\partial}{\partial y}(\kappa(T)\frac{\partial T}{\partial y})-\frac{\partial q_r}{\partial y}\right), \tag{3}$$

$$u=L_1\left(\frac{\partial u}{\partial y}\right), \quad v=v_w; \quad T=T_w+D_1\left(\frac{\partial T}{\partial y}\right); \qquad \text{at} \quad y=0, \tag{4}$$

$$u\rightarrow U_\infty, \quad T\rightarrow T_\infty, \qquad \text{as} \quad y\rightarrow\infty. \tag{5}$$

In the above equations u and v are the velocity components in x and y directions, ρ is the fluids density, τ_{xy} is the shear stress tensor, A is the permeability, σ is the electrical conductivity, B is the applied magnetic field, T is the temperature, C_p is the specific heat, κ is the variable thermal conductivity, q_r is the radiative heat flux, L_1 is the velocity slip factor, D_1 is the thermal slip factor and v_w describe suction/blowing through the porous plate. The shear stress component τ_{xy} for the power-law model, as derived by Bird *et al.* [36] is

$$\tau_{xy}=K\left|\frac{\partial u}{\partial y}\right|^{n-1}\frac{\partial u}{\partial y}. \tag{6}$$

Here K is the consistency coefficient and n is the power-law index. In Eq. (6) $n=1$ represents the Newtonian behaviour of the fluid and for $n<1$ behaviour of the fluid is known as shear-thinning which is categorized by an apparent viscosity which decrease with increase in shear rate. In case of $n>1$ fluid behaviour is called shear-thickening and characterized by an apparent viscosity which increases with increase in shear rate (details in [37]). Therefore a single parameter n describes the nature of fluid behaviour. Substitution of Eq.(6) in Eq.(2) gives

$$u\frac{\partial u}{\partial x}+v\frac{\partial u}{\partial y}=\frac{1}{\rho}\frac{\partial}{\partial y}\left(K\left|\frac{\partial u}{\partial y}\right|^{n-1}\frac{\partial u}{\partial y}\right)-\frac{1}{\rho A}(u-U_\infty)-\frac{\sigma B^2}{\rho}(u-U_\infty). \tag{7}$$

Following Das [35], we consider the temperature-dependent thermal conductivity and radiative heat flux of the form

$$\kappa=\kappa_\infty(1+\epsilon\frac{T-T_\infty}{\Delta T}), \qquad q_r=-\frac{16T_\infty^3\sigma^*}{3k^*}\frac{\partial T}{\partial y}, \tag{8}$$

where ϵ is the thermal conductivity parameter, κ_∞ is the thermal conductivity at ambient temperature and $\Delta T = T_w - T_\infty$, σ^* is the Stefan-Boltzmann constant and k^* is the mean absorption coefficient. Substitution of Eq. (8) into Eq. (3) gives

$$u\frac{\partial T}{\partial x} + v\frac{\partial T}{\partial y} = \frac{1}{\rho C_p}\left(\frac{\partial}{\partial y}\left(\kappa_\infty\left(1+\epsilon\frac{T-T_\infty}{T_w-T_\infty}\right)\frac{\partial T}{\partial y}\right) + \frac{16T_\infty^3\sigma^*}{3k^*}\frac{\partial^2 T}{\partial y^2}\right). \tag{9}$$

3 Method of Solution

In this section we transform the system of equations (1), (7) and (9) along with the boundary conditions (4)-(5) into a dimensionless form. For this purpose, the dimensionless stream function $\psi(x, y)$ of the form

$$u = \frac{\partial \psi}{\partial y}, \qquad v = -\frac{\partial \psi}{\partial x}, \tag{10}$$

identically satisfies the continuity Eq. (1). Using Eq. (10), Eqs. (7) and (9) becomes

$$\frac{\partial \psi}{\partial y}\frac{\partial^2 \psi}{\partial x \partial y} - \frac{\partial \psi}{\partial x}\frac{\partial^2 \psi}{\partial y^2} = \frac{1}{\rho}\left(\frac{\partial}{\partial y}\left[K\left|\frac{\partial^2 \psi}{\partial y^2}\right|^{n-1}\frac{\partial^2 \psi}{\partial y^2}\right] - \left(\frac{1}{\rho k} + \frac{\sigma B^2}{\rho}\right)\left(\frac{\partial \psi}{\partial y} - U_\infty\right)\right), \tag{11}$$

$$\frac{\partial \psi}{\partial y}\frac{\partial T}{\partial y} - \frac{\partial \psi}{\partial x}\frac{\partial T}{\partial x} = \frac{1}{\rho C_p}\left(\frac{\partial}{\partial y}\left(\kappa_\infty\left(1+\epsilon\frac{T-T_\infty}{T_w-T_\infty}\right)\frac{\partial T}{\partial y}\right) + \frac{16T_\infty^3\sigma^*}{3k^*}\frac{\partial^2 T}{\partial y^2}\right). \tag{12}$$

The boundary conditions are likewise transformed into

$$\frac{\partial \psi}{\partial y} = L_1\frac{\partial^2 \psi}{\partial y^2}, \quad \frac{\partial \psi}{\partial x} = -v_w, \quad T = T_w + D_1\left(\frac{\partial T}{\partial y}\right) \quad \text{at} \quad y = 0, \tag{13}$$

$$\frac{\partial \psi}{\partial y} \to U_\infty, \quad T \to T_\infty \quad \text{as} \quad y \to \infty, \tag{14}$$

where $L_1 = L\frac{U_\infty \rho}{K}\left(\frac{Kx}{\rho U_\infty^{2-n}}\right)^{\frac{1}{n+1}}$ is the velocity slip factor and $D_1 = D\frac{U_\infty \rho}{K}\left(\frac{Kx}{\rho U_\infty^{2-n}}\right)^{\frac{1}{n+1}}$ is the thermal slip factor with L and D are the initial values of velocity and thermal slip parameters respectively.

We introduce the following dimensionless similarity variable η, dimensionless stream function $\psi(\eta)$ and dimensionless temperature $\theta(\eta)$ of the form

$$\eta = \left(\frac{Re}{x/L}\right)^{\frac{1}{n+1}}\frac{y}{L}, \quad \psi(x,y) = LU_\infty\left(\frac{x/L}{Re}\right)^{\frac{1}{n+1}} f(\eta), \quad \theta(\eta) = \frac{T-T_\infty}{T_w-T_\infty}, \tag{15}$$

where $Re = \rho U_\infty^{2-n}L^n/K$ is the generalized Reynolds number. Using Eq. (15) into Eqs. (11)-(12), we obtain the self-similar system of ordinary differential equations along with the boundary conditions:

$$n|f''|^{n-1}f''' + \frac{1}{n+1}ff'' - (k+M)(f'-1) = 0, \tag{16}$$

$$\theta'' + \frac{P_{r\infty}}{(n+1)(1+\epsilon\theta+N_r)}f\theta' + \frac{\epsilon}{(1+\epsilon\theta+N_r)}\theta'^2 = 0, \tag{17}$$

$$f(\eta) = S, \quad f'(\eta) = \delta f''(\eta), \quad \theta(\eta) = 1 + \beta\theta'(\eta), \quad at \quad \eta = 0, \tag{18}$$

$$f'(\eta) \to 1, \quad \theta(\eta) \to 0, \quad as \quad \eta \to \infty. \tag{19}$$

In Eqs.(16)-(19), k is the permeability parameter, M is the magnetic parameter, $P_{r\infty}$ is the local Prandtl number, N_r is the thermal radiation parameter, S is the suction/blowing parameter corresponds to suction when $S > 0$ and corresponds to blowing when $S < 0$. Here δ and β

are the dimensionless velocity and thermal slip parameters respectively. These parameters are further defined as

$$k = \frac{x}{\rho A U_\infty}, \qquad M = \frac{x\sigma B^2}{\rho U_\infty}, \qquad N_r = \frac{16T_\infty^3\sigma^*}{3k^*\kappa_\infty}, \qquad S = -v_w\frac{x(n+1)}{U_\infty}\left(\frac{\rho U_\infty^{2-n}}{K}\right)^{\frac{1}{n+1}},$$

$$\delta = L\frac{U_\infty\rho}{K}, \qquad \beta = D\frac{U_\infty\rho}{K}, \qquad P_{r\infty} = \frac{C_p}{\kappa_\infty}K^{2/n+1}\left(\frac{U_\infty^3\rho}{x}\right)^{\frac{n-1}{n+1}} = (1+\epsilon\theta)P_r, \tag{20}$$

where $P_r = \frac{C_p}{\kappa}\left(\frac{U_\infty^3\rho}{x}\right)^{\frac{n-1}{n+1}} K^{2/n+1}$ is the Prandtl number. Using last equation of (20), Eq.(17) become

$$\theta'' + \frac{(1+\epsilon\theta)}{(1+\epsilon\theta+N_r)}\frac{P_r}{n+1}f\theta' + \frac{\epsilon}{(1+\epsilon\theta+N_r)}\theta'^2 = 0. \tag{21}$$

The nonlinear coupled ordinary differential equations (16) and (21) together with boundary conditions (18)-(19) are solved numerically using the Matlab bvp4c solver. In order to use bvp4c, we first convert these equations into a system of first order ordinary differential equations, that is,

$$f' = p, \quad p' = q, \quad q' = \frac{k+M}{n}\frac{p-1}{q^{n-1}} - \frac{fq^{2-n}}{n(n+1)}, \tag{22}$$

$$\theta' = z, \quad z' = -\frac{P_r}{n+1}\frac{1+\epsilon\theta}{(1+\epsilon\theta+N_r)}f\theta' - \frac{\epsilon}{(1+\epsilon\theta+N_r)}\theta'^2, \tag{23}$$

$$f(\eta) = S, \quad p(\eta) = \delta q(\eta), \quad at \quad \eta = 0, \quad p(\eta) \to 1 \quad as \quad \eta \to \infty \tag{24}$$

$$\theta(\eta) = 1 + \beta z(\eta), \quad at \quad \eta = 0; \quad \theta(\eta) \to 0 \quad as \quad \eta \to \infty. \tag{25}$$

The bvp4c code need an initial guess for $q(\eta)$ and $z(\eta)$ at $\eta = 0$, and through collocation method we vary each guess until we obtain an appropriate solution for our problem. We verify the accuracy of these solutions by comparing them with those found using shooting method. The result for the velocity profile with $M = 0$ and $n = 1$ (i.e in the absence of MHD and for the case of Newtonian fluids) are compared with the available published results of Bhattacharyya *et al.* [38]. The comparison is presented in figure (2).

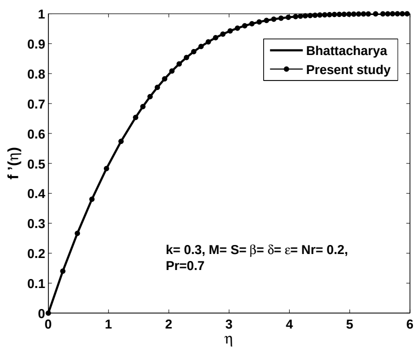

Figure 2: Velocity profile $f'(\eta)$ for magnetic parameter $M = 0$ and power-law index $n = 1$.

4 Results and Discussion

In this section we discuss the numerical results presented in the form of graphs and tables. The computations are performed for several values of power-law index n and the effects of velocity slip parameter δ, thermal slip parameter β, permeability parameter k, magnetic parameter M, suction/injection parameter S, Prandtl number P_r, variable thermal conductivity ϵ and thermal radiation N_r on velocity and temperature profile are discussed.

In figure (3) the effect of velocity slip parameter δ on the velocity profile of Newtonian, shear thinning and shear thickening fluids are presented. The comparison of curves with same power-law index show that the increase in the velocity slip at the boundary, increase the fluid velocity within the boundary layer. This is due to the positive value of the fluid velocity adjacent to the surface. Moreover, the increase in magnitude of the slip parameter allows more fluid to slip past the plate and accordingly the flow through the boundary layer will increase.

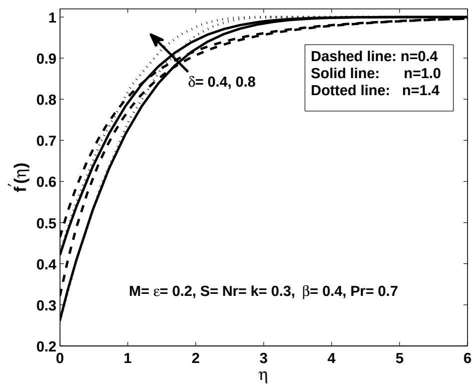

Figure 3: Velocity $f'(\eta)$ profiles for different values of slip parameter δ and power-law index n.

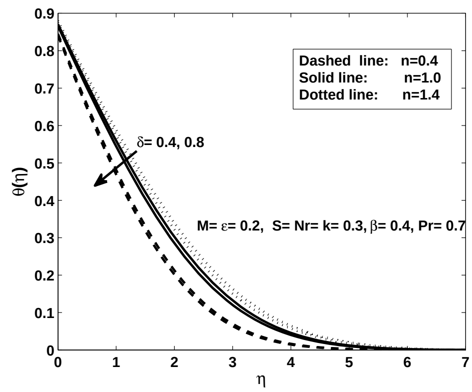

Figure 4: Temperature $\theta(\eta)$ profiles for different values of slip parameter δ and power-law index n.

It is important to note that temperature is dependent on velocity in situations where heat transfer is accomplished by convection, as this principle will also be important for following discussions. In figure (4) the temperature profile $\theta(\eta)$ is plotted for two different values of velocity slip parameter δ. It is observed that the increase in the magnitude of velocity slip at boundary enhance the rate of heat transfer.

Figures (3)-(4) with slip parameter $\delta = 0.8$ gives variation of velocity and thermal profiles for both Newtonian and non-Newtonian fluids. It is evident from figure (3), initially the velocity of shear-thinning fluids $n < 1$ rises fastest, followed by the shear-thickening fluids $n > 1$ and then the Newtonian fluid $n = 1$. This is due to smallest effective viscosity of shear thinning fluids at that point. Therefore shear thinning fluids achieve a higher strain rate and velocity. Whereas at later times the velocity of shear thinning fluids, first decrease below the shear thickening fluids and then the Newtonian fluid. This opposite trend is observed due the decrease in shear stress and increase in the viscosity of the shear thinning fluids. Furthermore, figure (4) show the thickness of thermal boundary layer is relatively thin for shear thinning fluid $n < 1$ (f approaches zero quickly). However, if $n > 1$ the boundary layer is relatively thick.

The effect of thermal slip parameter β on temperature profile is presented in figure (5). The increase in thermal slip parameter decreased the fluid temperature for a given distance from the plate. This is due to the fluid adjacent to the surface of the plate having temperature lower than that of the plate. Figure (6) illustrates the effect of thermal radiation parameter N_r on temperature profiles. We see that an increase in thermal radiation parameter increase the thickness of thermal boundary layer. From figure (6) it is also noticed, the thickness of thermal boundary layer increase with increase in power-law index n.

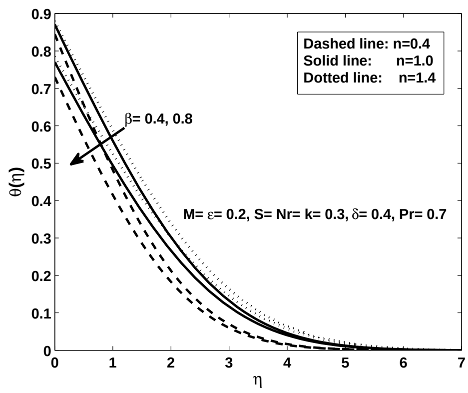

Figure 5: Temperature $\theta(\eta)$ profiles for different values of thermal slip parameter β and power-law index n.

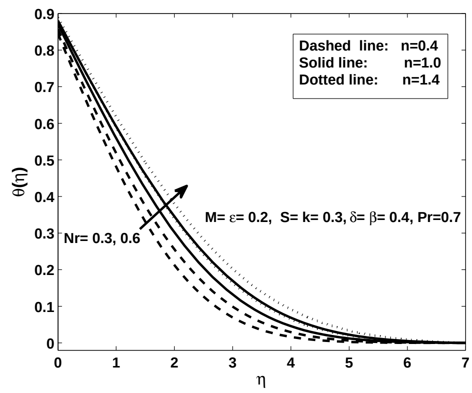

Figure 6: Temperature $\theta(\eta)$ profile for different values of thermal radiation parameter N_r and power-law index n.

In figure (7) effect of variation in permeability on fluid velocity with slip condition is shown. It is noticed that the velocity of the fluid across the boundary layer increase with increase in the permeability of the porous medium. In other words, the increase in porosity of the medium decrease the magnitude of Darcian body force which enhances the motion of the fluid in the boundary layer and ultimately decelerates the fluid particles in the porous medium. The partial slip and the effect of variation in permeability on temperature profile is presented in figure (8). It is observed that the increase in permeability enhanced the heat transfer rate and decrease the thickness of thermal boundary layer.

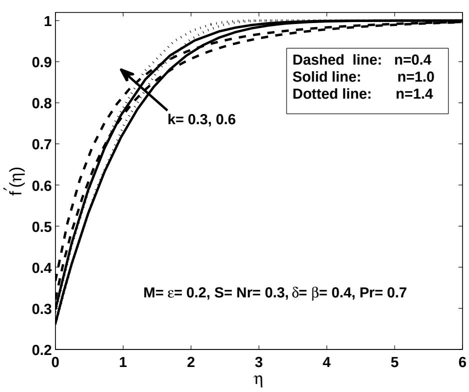

Figure 7: Velocity $f'(\eta)$ profiles for different values of permeability parameter k and power-law index n.

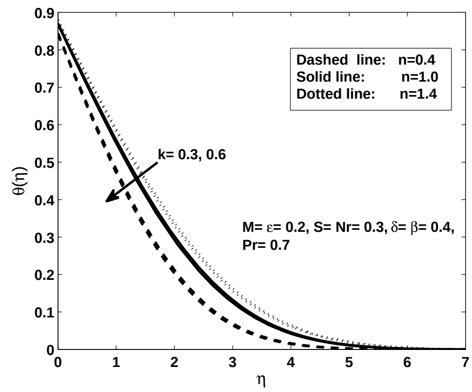

Figure 8: Temperature $\theta(\eta)$ profiles for different values of permeability parameter k and power-law index n.

Figure (7) with permeability $k = 0.3$ and different values of power-law index give variation of velocity profiles for Newtonian and non-Newtonian fluids. It is evident from figure (7), initially the shear-thinning fluid rises faster when compared with the shear-thickening fluid. This is due to smallest effective viscosity of shear thinning fluids. Whereas the opposite trend is observed at the later times as viscosity of the shear thickening fluid will decrease. Moreover, the slip condition at the boundary allows more fluid flow past the plate and decrease the thickness of boundary layer.

The effects of MHD parameter M on fluid velocity and temperature under slip condition is shown in figures (9)-(10). It is clear that the variation in MHD parameter M show the similar effect as variation in permeability parameter k, i.e., the increase in magnetic field causes to increase in velocity of the fluid and the rate of heat transfer.

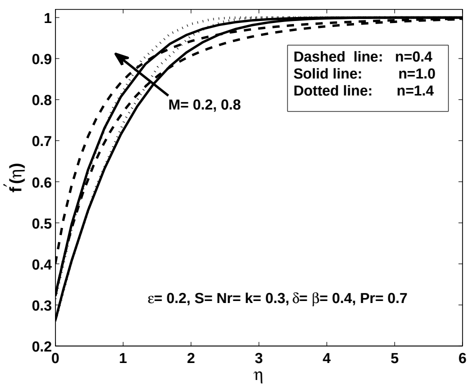

Figure 9: Velocity $f'(\eta)$ profiles for different values of magnetic parameter M and power-law index n.

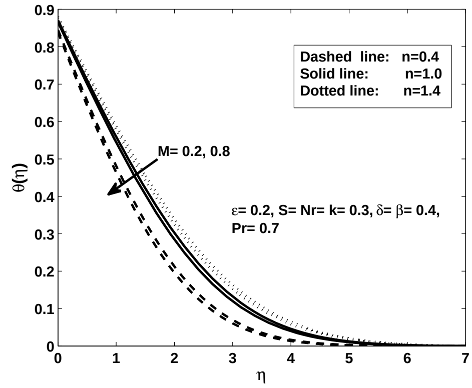

Figure 10: Temperature $\theta(\eta)$ profiles for different values of magnetic parameter M and power-law index n.

Figures (11)-(12) depicted the affect of suction/injection parameter S on velocity and temperature profiles in the presence of slip condition and magnetic field for porous plate in a porous medium. It is clear from the figures that suction $S > 0$ caused an increase in fluid velocity as more fluid is sucked through the porous wall and reduce the thickness of momentum boundary layer. Opposite behaviour is observed for $S < 0$. In case of temperature distribution through the boundary layer, the thermal boundary layer thickness decreases with increasing values of $S > 0$. This will increase the rate of heat transfer through the boundary layer.

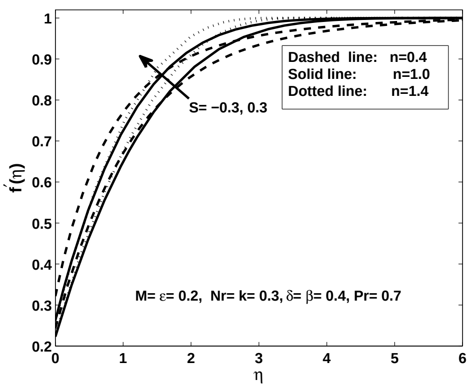

Figure 11: Velocity $f'(\eta)$ profiles for different values of suction/injection parameter S and power-law index n.

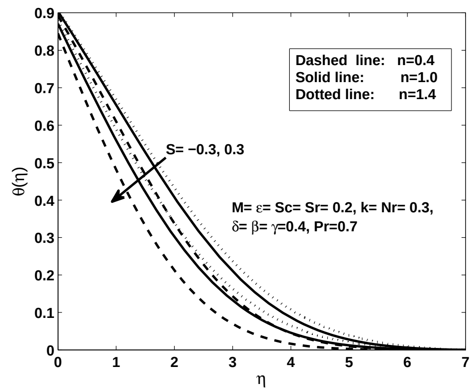

Figure 12: Temperature $\theta(\eta)$ profiles for different values of suction/injection parameter S and power-law index n.

Prandtl number is defined as the ratio of momentum diffusivity to thermal diffusivity. Variation in Prandtl number and its effects on temperature profiles is shown in figure (13). It is observed that the temperature of the power-law fluid decrease with increasing values of the Prandtl number under slip condition. This trend is consistent with the fact that increase in Prandtl number will increase the fluid viscosity within the boundary layer. This will cause a decrease in the velocity flow and the decrease in temperature. The temperature profiles for various values of thermal conductivity parameter ϵ is shown in figure(14). It is noticed, an increase in thermal conductivity parameter increase the fluid temperature across the boundary layer. It would also increase the thermal boundary layer thickness.

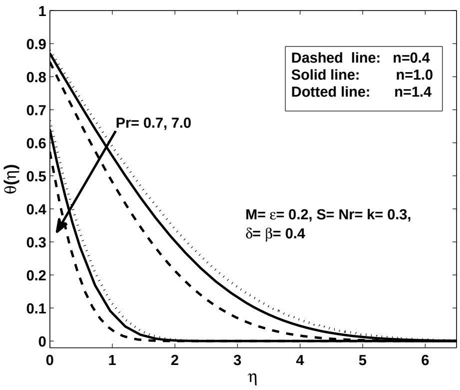

Figure 13: Temperature $\theta(\eta)$ profile for different values of Prandtl number Pr and power-law index n.

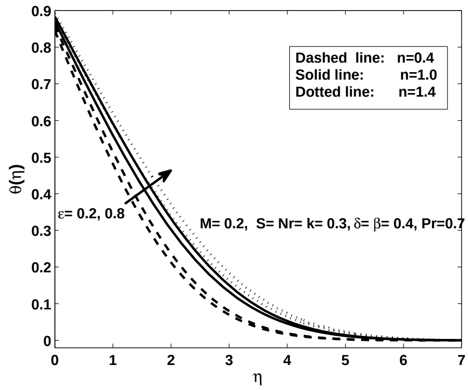

Figure 14: Temperature $\theta(\eta)$ profile for different values of thermal conductivity parameter ϵ and power-law index n.

Table (1) presented the nature of skin friction coefficient for different physical parameters. It is observed; the shear thinning fluids have the highest value of skin friction coefficient followed by the Newtonian fluid and then the shear thickening fluids. This is because of the rate of increase in velocity at the surface of porous plate is highest for shear thinning fluids. Moreover, the skin friction coefficient decrease with increase in slip parameter δ and increase with increase in magnetic parameter M and permeability parameter k. The increasing values of skin friction coefficient correspond to thinning of velocity boundary layer. Whereas the decreasing values of skin friction coefficient corresponds to fluid velocity at the surface approaching to free stream velocity.

n	k	M	δ	$f''(0)$
0.4	0.3	0.6	0.3	1.036
1.0				0.8114
1.4				0.7861
1.4	0.3	0.6	0.3	0.7861
	0.6			0.8629
	0.8			0.9001
1.4	0.3	0.2	0.3	0.6718
		0.6		0.7861
		1.0		0.8712
1.4	0.3	0.6	0.0	0.9667
			0.3	0.7861
			0.6	0.656

Table 1: Values of the skin friction coefficient $f''(0)$.

n	k	M	δ	β	P_r	N_r	$-\theta'(0)$
0.4	0.3	0.2	0.3	0.3	0.7	0.2	0.3879
1.0							0.3231
1.4							0.3006
1.4	0.6	0.2	0.3	0.3	0.7	0.2	0.307
	0.8						0.3102
1.4	0.3	0.4	0.3	0.3	0.7	0.2	0.3052
		0.8					0.3116
1.4	0.3	0.2	0.6	0.3	0.7	0.2	0.3127
			0.8				0.3186
1.4	0.3	0.2	0.3	0.6	0.7	0.2	0.2768
				0.8			0.2629
1.4	0.3	0.2	0.3	0.3	3.0	0.2	0.5659
					7.0		0.8234
1.4	0.3	0.2	0.3	0.3	0.7	0.4	0.2846
						0.8	0.2603

Table 2: Values of the Nusselt number $-\theta'(0)$

Nusselt number is the ratio of convective to conductive heat transfer at the surface of the plate. In table (2) different values of Nusselt number are presented when all other parameters are kept constant. It is observed that the Nusselt number decrease with increase in power-law index n. This observation is consistent with the fact that the decrease in surface temperature is slowest for shear thickening fluids. It is noticed from the table that an increase in the permeability parameter k, magnetic parameter M and Prandtl number P_r results in increase of the Nusselt number. Moreover, the increase in the slip parameters δ, β and the thermal radiation parameter N_r has the effect of lowering the Nusselt number. The effect of increase in Nusselt number is analogous to an increase in heat transfer rate and the thinning of thermal boundary layer.

5 Conclusion and Future Work

In this article, we studied the MHD slip flow and heat transfer of power law fluid over a porous flat plate with variable thermal conductivity and thermal radiation. The velocity and thermal slip conditions are employed and thermal conductivity is considered as linear function of temperature. The governing boundary layer equations along with the boundary conditions were transformed into a coupled system of nonlinear ordinary differential equations using similarity transformation. The resulting system differential equations were solved numerically using Matlab bvp4c code and results are presented in the form of graphs and tables. We have summarized our results based on the key parameters such as, thermal conductivity paramter, thermal radiation parameter, permeability parameter, velocity and thermal slip parameters, injection and suction parameters and Prandtl number along with variation of the power law index n.

The present model has exploited a number of simplifications in order to focus on the principal effects of slip parameter and power-law index and temperature dependent thermal conductivity. An interesting area to explore in future investigations would be the use of temperature dependent viscosity, variable porosity, heat flux and convective boundary conditions, multidimensional MHD slip flow and heat transfer of non-Newtonian fluids, coupled fluid models and structure interactions. Alternatively, the nonlinear coupled ordinary differential equations (16) and (21) together with boundary conditions (18)-(19) can be solved by employing the semi-analytical methods [39]. Clearly there is an opportunity for experimental work on these systems.

References

[1] L. Prandtl, "Uber flussigkeitsbewegungen bei sehr kleiner reibung," *Intern. Math. Kongr. Heidelberg*, pp. 484–491, 1904.

[2] H. Blasius, "Grenzschichten in flüssigkeiten mit kleiner reibung," *Zeitschrift für angewandte Mathematik und Physik (ZAMP)*, vol. 56, pp. 1–37, 1908.

[3] J. Pascal and H. Pascal, "Some similarity solutions to shear flows of non-newtonian power law fluids," *Acta Mechanica*, vol. 112, pp. 229–236, 1994.

[4] A. Abussita, "A note on a certain boundary layer equation," *Applied Mathematics and Computation*, vol. 64, pp. 73–77, 1994.

[5] A. Ishak, "Similarity solutions for fow and heat transfer over a permeable surface with convective boundary conditions," *Applied Mathematics and Computation*, vol. 217, pp. 837–842, 2010.

[6] E. Magyari, "Comment on similarity solution for laminar thermal boundary layer flow over a flat plate with a convective surface boundary condition by a. aziz," *Communications in Nonlinear Science and Numerical Simulation*, vol. 16, pp. 599–601, 2011.

[7] K. Vafai, *Handbook of Porous Media.* New York: Marcel Dekker, 2000.

[8] D. Ingham and I. Pop, *Transport Phenomena in Porous Media.* New York: Pergamon, Elsevier, 1998.

[9] M. Kumari, I. Pop, and G. Nath, "Non-darcian effects on forced convection heat transfer over a flat plate in a highly porous medium," *Acta Mechanica*, vol. 84, pp. 201–207, 1990.

[10] N. Luna and F. Mndez, "Forced convection on a heated horizontal flat plate with finite thermal conductivity in a non-darcian porous medium," *International Journal of Thermal Sciences*, vol. 44, pp. 656–664, 2005.

[11] A. Khaled and K. Vafai, "The role of porous media in modeling flow and heat transfer in biological tissues," *International Journal of Heat and Mass Transfer*, vol. 46, pp. 4989–5003, 2003.

[12] O. Makinde, "Free convection flow with thermal radiation and mass transfer past a moving porous plate.," *International Communications in Heat Mass Transfer*, vol. 32, pp. 1411–1419, 2005.

[13] F. Ibrahim, A. Elaiw, and A. Bakr, "Influence of viscous dissipation and radiation on unsteady mhd mixed convection flow of micropolar fluids.," *Applied Mathematics and Information Sciences*, vol. 2, pp. 143–162, 2008.

[14] M. A. P. Datti and N.Mahesha, "Flow and heat transfer in a power-law fluid over a stretching sheet with variable thermal conductivity and non-uniform heat source," *International Journal of Heat and Mass Transfer*, vol. 52, pp. 2901–2913, 2009.

[15] J. Luk, R. Mutharasan, and D. Apelian, "Experimental observations of wall slip: tube and packed bed flow," *Industrial and Engineering Chemistry Research*, vol. 26, p. 16091616, 1987.

[16] D. Kalyon, "Apparent slip and viscoplasticity of concentrated suspensions," *Journal of Rheology*, vol. 49, p. 621640, 2005.

[17] G. Beavers and D. Joseph, "Boundary conditions at a naturally permeable wall," *Journal of Fluid Mechanics*, vol. 30, pp. 197–207, 1967.

[18] H. Andersson, "Slip flow past a stretching surface," *Acta Mechanica*, vol. 158, pp. 121–125, 2002.

[19] A. Farhad, M. Norzieha, S. Sharidan, and I. Khan, "On accelerated mhd flow in a porous medium with slip condition," *European Journal of Scientific Research*, vol. 57, pp. 293–304, 2011.

[20] M. Martin and I. Boyd, "Momentum and heat transfer in laminar boundary layer with slip flow," *Journal of Thermophysics and Heat Transfer*, vol. 20, pp. 710–719, 2006.

[21] A. Aziz, J. Siddique, and T. Aziz, "Steady boundary layer slip flow along with heat and mass transfer over a flat porous plate embedded in a porous medium," *PLOS ONE*, 2014.

[22] C. Cheng, "Soret and dufour effects on free convection boundary layers of non-newtonian power law fluids with yield stress in porous media over a vertical plate with variable wall heat and mass fluxes," *International Communications in Heat and Mass Transfer*, vol. 38, pp. 615–619, 2011.

[23] J. Loureiro and A. Freire, "Asymptotic analysis of turbulent boundary-layer flow of purely viscous non-newtonian fluids," *Journal of Non-Newtonian Fluid Mechanics*, vol. 199, pp. 20–28, 2013.

[24] I. Baoku, B. Olajuwon, and A. Mustapha, "Heat and mass transfer on a mhd third grade fluid with partial slip flow past an infinite vertical insulated porous plate in a porous medium," *International Journal of Heat and Fluid Flow*, pp. 81–88, 2013.

[25] A. Acrious, M. Shah, and E. Peterson, "Momentum and heat transfer in laminar boundary layer flow on non-newtonian fluids past external surfaces," *AIChE Journal*, vol. 6, pp. 312–316, 1960.

[26] W. Schowalter, "The application of boundary layer theory to power law pseudo plastic fluids: similar solutions," *AIChE Journal*, vol. 6, 1960.

[27] H. Andersson, K. Bech, and B. Dandapat, "Magnetohydrodynamic flow of a power law fluid over a stretching sheet," *International Journal of Non-Linear Mechanics*, vol. 72, no. 4, pp. 929–936, 1992.

[28] M. Hajmohammadi and S. Nourazar, "On the insertion of a thin gas layer in micro cylindrical couette flows involving power-law liquids," *International Journal of Heat and Mass Transfer*, vol. 75, pp. 97–108, 2014.

[29] M. Hajmohammadi, S. Nourazar, and A. Campo, "Analytical solution for two-phase flow between two rotating cylinders filled with power law liquid and a micro layer of gas," *Journal of Mechanical Science and Technology*, vol. 28, pp. 1849–1854, 2014.

[30] D. Pal and S. Chatterjee, "Soret and dufour effects on MHD convective heat and mass transfer of a power-law fluid over an inclined plate with variable thermal conductivity in a porous medium," *Applied Mathematics and Computation*, vol. 219, pp. 7556–7574, 2013.

[31] T. Hayat, M. Hussain, A. Alsaedi, S. Shehzad, and G. Chen, "Flow of power-law nanofluid over a stretching surface with newtonian heating," *Journal of Applied Fluid Mechanics*, vol. 8, pp. 273–280, 2015.

[32] H. Duwairi and R. Damseh, "Mhd-buoyancy aiding and opposing flows with viscous dissipation effects from radiate vertical surfaces," *Canadian Journal of Chemical Engineering*, vol. 82, p. 613, 2004.

[33] M. Alam, M. Rahman, and M. Sattar, "On the effectiveness of viscous dissipation and joule heating on steady magnetohydrodynamic heat and mass transfer flow over an inclined radiate isothermal permeable surface in the presence of thermophoresis," *Commun Nonlinear Sci Numer Simul*, vol. 14, p. 2132, 2009.

[34] M. Rahman and K. Salahuddin, "Study of hydromagnetic heat and mass transfer flow over an inclined heated surface with variable viscosity and electric conductivity," *Commun Nonlinear Sci Numer Simulat*, vol. 15, pp. 2073–2085, 2010.

[35] K. Das, "Slip effects on heat and mass transfer in mhd micropolar fluid flow over an inclined plate with thermal radiation and chemical reaction," *International Journal of Numerical Methods in Fluids*, vol. 70, pp. 96–113, 2012.

[36] R. Bird, W. Stewart, and E. lightfoot, *Transport Phenomena*. New York: John Wiley, 1960.

[37] R. Chhabra and J. Richardson, *Non-Newtonian Flow and Applied Rheology: Engineering Applications*. Oxford: Butterworth-Heinemann, second edition ed., 2008.

[38] K. Bhattacharyya, S. Mukhopadhyay, and G. Layek, "Steady boundary layer slip flow and heat transfer over a flat porous plate embedded in a porous media," *Journal of Petroleum Science and Engineering*, vol. 78, pp. 304–309, 2011.

[39] M. Hajmohammadi and S. Nourazar, "On the solution of characteristic value problems arising in linear stability analysis; semi analytical approach," *Applied Mathematics and Computation*, vol. 239, pp. 126–132, 2014.

Paper submitted: August 25, 2015
Paper revised: February 24, 2016
Paper accepted: February 26, 2016